Electronic Supplementary Material (ESI) for Soft Matter.

SUPPLEMENTARY INFORMATION

Total Balance of Forces

Instead of using Young's relation to derive Equation (1), we can use total equilibrium of forces to obtain the same result. The total force per unit of line applied at the interface between two cylinders is $p \times 2\ell$ where $\ell = [(d + r) - r\cos\alpha]$ (see Fig. S1) is the projected cross section of the liquid vapor interface. The applied pressure must be balanced by the forces at the contact point A and A' that have a total vertical component $2\gamma_{lv}\sin\beta$, where $\beta = \theta_c - (\pi/2 - \alpha)$ is the angle between the interface and the horizontal direction. It gives

$$p \times 2[(d + r) - r\cos\alpha] = 2\gamma_{lv}\sin\beta \longrightarrow p = \frac{\gamma_{lv}}{r}\frac{\cos(\theta_c + \alpha)}{\cos\alpha - D_*}$$

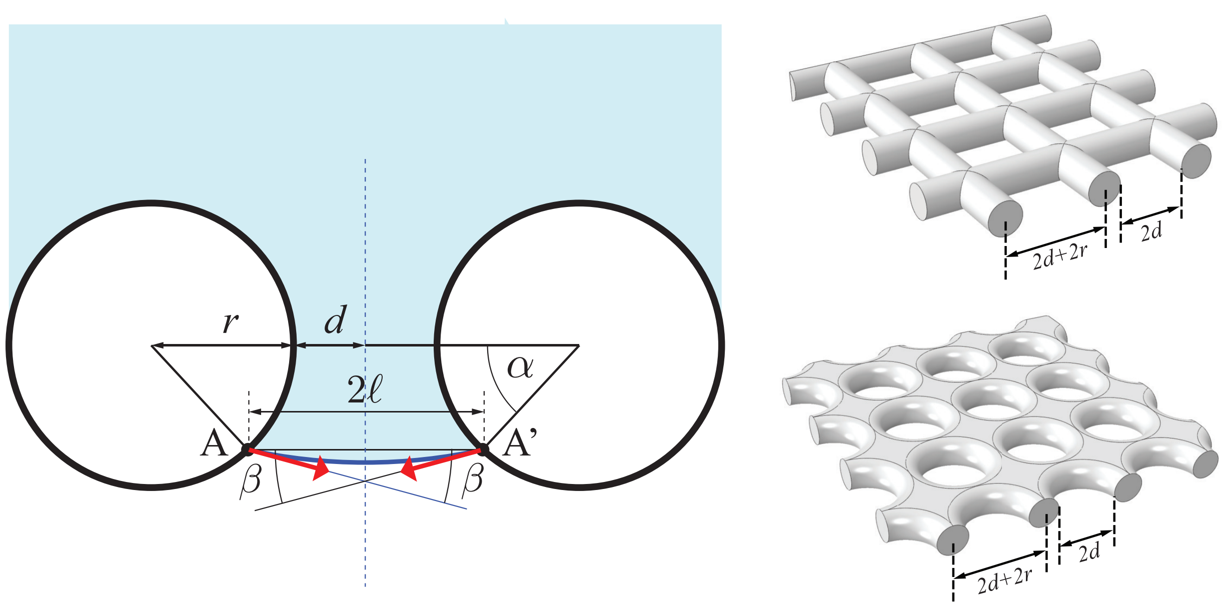

Fig. S 1. Left: Schematic of the vapor liquid interface between two cylinders of radius r and their axes a distance $2(d + r)$ apart. Right: This exact configuration is observed for a mesh textured surface (upper right) or a surface textured by pores of double curvature (bottom right).

Similar calculation can be made for a pore textured surface with geometry defined by Fig. S1. The total pressure applied to the interface is pS where $S = \pi\ell^2$ is the projected area of the liquid vapor interface. The pressure must be balanced by the vertical forces at the line of contact $\gamma_{lv} \sin\beta 2\pi\ell$. It gives

$$p \times \pi[(d+r) - r\cos\alpha]^2 = 2\pi\gamma_{lv}\sin\beta[(d+r) - r\cos\alpha] \longrightarrow p = 2\frac{\gamma_{lv}}{r}\frac{\cos(\theta_c+\alpha)}{\cos\alpha - D_*}$$

Thus, except for a factor 2 the pressure for a pore structured topography is equivalent to the pressure in a mesh topography.

Measurement of the contact angle and data fit

Cassie and Baxter[S1] addressed the problem of enhanced hydrophobicity studying the contact angle of large water drops on a porous surface made of wax parallel filaments. Using a two dimensional geometry, they showed that the apparent angle θ_* is connected with the dimensionless spacing ratio D_* and the contact angle θ_c of the water drop measured on a flat surface coated with the same wax. The apparent angle is predicted by the Cassie Baxter relation

$$\cos\theta_* = f_1\cos\theta_c - f_2 \qquad \text{(S 1)}$$

where f_1 and f_2 are

$$f_1 = \frac{(\pi-\theta_c)}{D_*} \qquad \text{(S 2)}$$

$$f_2 = 1 - \frac{\sin\theta_c}{D_*} \qquad \text{(S 3)}$$

An important assumption of this relation is that the pressure inside the water drop is almost zero so that the water-vapor interface is flat. This happens for $\alpha = \pi/2 - \theta_c$ in Fig. S1.

Equation (S 1) is used to predict the apparent contact angle in terms of θ_c and D_*; however, here we use it in the inverse way: the apparent contact angle of a large water drop is measured for a mesh of known value of D_*, and then the contact angle is obtained by solving Eq. (S 1). This procedure give us a method to estimate the contact angle of the solid part of the mesh without having to prepare a smooth surface to study the contact angle of the solid. Figure S2 (and the inset of Fig. 6) gives the measured value of θ_* for the set of meshes used in our experiments. Although we observe a large variation in the measure apparent angle from 90 to 120 degrees, the contact angle extracted from this measurements has a narrow variation from 59 to 63 degrees. The average value is $\theta_c = 62^o$.

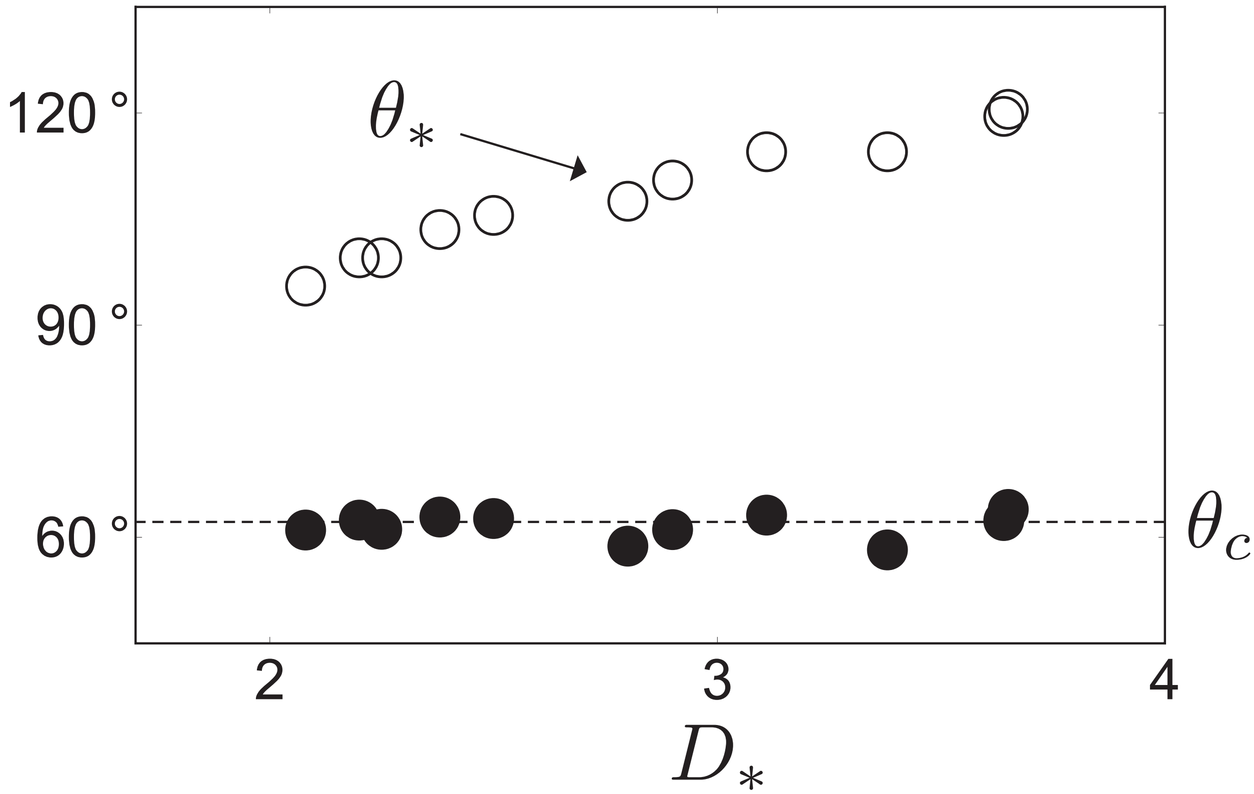

Fig. S 2. The measured apparent contact angle θ_* as a function of the dimensionless spacing ratio (open circles). The black circles give the predicted contact angle θ_c for each experiment by using Eq. (S 1)

There have been some criticism to Eq. (S 1) in recent studies because it is derived in terms of pure two dimensional arguments. Jiang et al.[S3] claim that Eq. (S 1) predict incorrect apparent angles for woven meshes with a large pore size (larger than a 100μm $\times$ 100μm). Similarly, Venkateshan and Tafreshi [S2] have reported numerical simulations that disagree with the prediction of Eq. (S 1) for large porous size and small water drops. We measured the apparent angle in large water drops to avoid these problems. In our case, a good validation of Eq. (S 1) is that all our measurements can be explained by a common constant parameter θ_c as it is observed in Fig. S2.

Equivalent analysis to obtain the angle of contact θ_c is made by studying the breakthrough pressure. For one layer of filaments this corresponds to leaking, and the critical pressure is predicted by the relation

$$p_B = \begin{cases} p_m = \frac{\gamma_{lv}}{r}\frac{1}{(D_*^2 - \sin^2\theta_c)^{1/2} + \cos\theta_c} & D_* < D_{\pi/2} = \tan\theta_c \\ p_{\pi/2} = \frac{\gamma_{lv}}{r}\frac{\sin\theta_c}{D_*} & D_* > D_{\pi/2} \end{cases}$$

It is noteworthy that the maximum pressure and saturation pressure conditions are continuously connected at $D_* = D_{\pi/2}$, hence, the regular behavior of p_m for $d \to 0$ is reflected in the regular behavior of $p_{\pi/2}$. The contact angle θ_c is the only free parameter in this relation and we use it to fit the data shown in Fig. 6. It gives $\theta_c \approx 57^o$ and a coefficient of determination R-squared 0.99.

The same fit can be applied to the prediction of Eq. 1 in the main text

$$p_B = \frac{\gamma_{lv}}{d}\frac{2r(1-\cos\theta_c)}{(d + 2r\sin\theta_c)}$$

It gives $\theta_c \approx 72^o$ with an R-squared of 0.87. Thus, the breakthrough pressure predicted in terms of the saturation and maximum pressure mechanisms is a better predictor of our observations.

Videos

We observe two types of behaviors when studying the breakthrough pressure in our experiments: 1) localized leaking driven by defects in the mesh where the breakthrough happens in particular places of the mesh where defects impose a local larger value of the spacing ratio, and 2) global leaking that happens in all parts of the mesh at the same time. They are shown in the following movies

- Video_S1a: side view of the setup showing localized leaking
- Video_S1b: bottom view of the setup showing localized leaking
- Video_S2a: side view of the setup showing global leaking
- Video_S2b: bottom view of the setup showing global leaking

[S1] A.B.D. Cassie and S. Baxter, *Trans. Faraday Soc.*, 1944, **40**, 546.

[S2] D.G. Venkateshan and H.V. Tafreshi, *Colloid and Surfaces A*, 2018, **538**, 310.

[S3] Z.X. Jiang, L. Geng, Y.D. Huang, S.A. Guan, W. Dong, and Z.Y. Ma, J. Colloid Interface Sci., 2011, **354**, 866.